

# Optical absorption and emission properties of Nd<sup>3+</sup> doped fluorophosphates glass for broadband fiber amplifier applications

J. H. Choi and F. G. Shi\*

Department of Chemical Engineering and Materials Science,  
University of California, Irvine, CA 92697-2575;

A. Margaryan and A. Margaryan  
AFO Research Inc, Glendale, CA 91209;

W. E. van der Veer  
Department of Chemistry, University of California, Irvine CA 92697-2025

## ABSTRACT

A new series of fluorophosphates glass is developed which can be doped with an extremely high concentration of Nd<sup>3+</sup>. The dopant concentration dependence of optical absorption and emission properties is reported here for the concentration range of  $2.5 \times 10^{20}$  to  $1.25 \times 10^{21}$  (ions/cm<sup>3</sup>). Absorption and emission measurements are performed in order to evaluate the spontaneous emission probability, absorption cross-section, emission cross-section, and laser performance parameters. The stimulated emission cross section for the  ${}^4F_{3/2} \rightarrow {}^4I_{13/2}$  transition increases from 1.14 to 1.64 ( $\times 10^4$  cm<sup>2</sup>) and for the  ${}^4F_{3/2} \rightarrow {}^4I_{11/2}$  transition from 3.68 to 6.68 ( $\times 10^4$  cm<sup>2</sup>) in the MBBA/NdI and the MBBA/NdII, respectively. The extraction efficiency was recorded in the range of 1.91 - 2.73 for  ${}^4F_{3/2} \rightarrow {}^4I_{13/2}$  and of 6.18 - 9.41 for  ${}^4F_{3/2} \rightarrow {}^4I_{11/2}$  for the MBBA/NdI and the MBBA/NdII, respectively. The new (Mg, Ba)F<sub>2</sub>-based fluorophosphates glass (MBBA system) is promising for broadband compact optical fiber and waveguide amplifier applications.

**Keyword:** *Spontaneous emission probability, Absorption cross-section, Emission cross-section, Fluorophosphates*

## 1. INTRODUCTION

Most of the potential laser host materials including silica glass are limited with respect to the maximum rare earth dopant concentration. In the case of silica glass, an Nd<sup>3+</sup> dopant concentration of greater than 2wt% is required to shorten the length of currently available active devices such as fiber amplifiers [1]. Thus, there is a strong need for new laser host

---

\* Frank G. Shi (correspondence): Email: [fgshi@uci.edu](mailto:fgshi@uci.edu); phone: 1 949 824 5362; fax: 1 949 824 2541

materials which can be doped with a relatively high R.E. dopant concentration. Among many potential laser host materials, fluorophosphates glasses show important advantages such as low phonon energy, transmittance from UV to IR spectral range, and low nonlinear refractive index [2-4]. Furthermore, an incorporation of metaphosphate compounds into fluoride leads to an extra room for rare earth ions this is because an incorporation of  $\text{Ba}(\text{PO}_3)_2$  and  $\text{Al}(\text{PO}_3)_3$ , could provide multiple sites for rare earth dopants.

The purpose of this paper is to report a new laser host material based on  $(\text{Mg}, \text{Ba})\text{F}_2$ . Major optical properties are determined from the absorption and the emission spectra to evaluate the performance of this new host material doped with  $\text{Nd}^{3+}$  for optical amplifier and laser application.

## 2. EXPERIMENTAL ARRANGEMENT

### 2.1 Glass synthesis

Starting materials from reagent-grade (City Chemicals) and  $\text{Er}_2\text{O}_3$  (Spectrum Materials) have above 99.99% purity. A series of glasses were weighed on 0.001% accuracy and mixed thoroughly. The raw mixed materials were melted in a vitreous carbon crucible in Ar-atmosphere at 1200-1250°C. Glass systems according to  $\text{Nd}^{3+}$  ion concentration are named MBBA/NdI ( $2.50 \times 10^{+20} \text{ cm}^{-3}$ ) and MBBA/NdII ( $6.26 \times 10^{+20} \text{ cm}^{-3}$ ). The quenched samples were annealed at transition temperature below 50-100°C to remove an internal stress. The residual stress was examined by the polariscope (Rudolph Instruments). Samples for optical and spectroscopic measurements were cut and polished by the size of  $15 \times 10 \times 2 \text{ mm}^3$ . The refractive index was measure by Abbe refractometer (ATAGO). The absorption spectra at room temperature were recorded in the range of 400-1700nm by Perkin-Elmer (Lambda 900). The emission spectra and fluorescence lifetime are measured by exciting the samples with the 800nm line of laser diode.

### 2.2 Spectral measurement

The absorption spectra were recorded at room temperature in the range of 400-1700 nm with a Perkin-Elmer photo spectrometer (Lambda 900). The resolution is set to 1 nm. Emission spectra are obtained by excitation of the samples with 808 nm radiation from a 1W CW Laser Diode (Coherent). The fluorescence radiation is then recorded over the range 900-1400 nm using a monochromator (Acton SpectraPro 300) and a Ge-photodiode (Thorlabs). The laser radiation incident to the sample is passed through an optical chopper (Stanford Research) enabling the use of a lock-in amplifier (Ametek 5105) to recover and amplify the electronic signal from the detector. The lifetime of the excited state is determined with a Q-switched Nd:YAG laser pumping an OPO (Continuum Surelite) tuned to 808 nm (Idler). The duration of the pulses is 5 ns. The fluorescent radiation is detected using a Si pin photodiode (Thorlabs) via an interference filter (Edmund Scientific). The signal is amplified with a recorded with a fast oscilloscope (LeCroy 9350) and transferred to a computer where it is fitted to an exponential.

### 3. RESULTS AND DISCUSSION

#### 3.1 Absorption properties

The absorption spectra with respect to  $\text{Nd}^{3+}$  dopant concentration are shown in Fig. 1. The spectra of  $\text{Nd}^{3+}$  ions in (Mg, Ba)  $\text{F}_2$ -based fluorophosphates (MBBA system) in the 400-950nm are corresponding to transitions from ground state  $^4I_{9/2}$  to various excited state. The average wavelength was taken to be the baricentres of the absorption bands. The absorption coefficient and mean wavelength can be used to calculate optical properties. The absorption peaks of  $\text{Nd}^{3+}$  ions in (Mg, Ba)  $\text{F}_2$ -based fluorophosphates are similar in their spectral features with a little bit difference in peak width and the relative intensity with  $\text{Nd}^{3+}$  concentration increases. The wavelength at each absorption peak was not shifted with respect to  $\text{Nd}^{3+}$  ion concentration

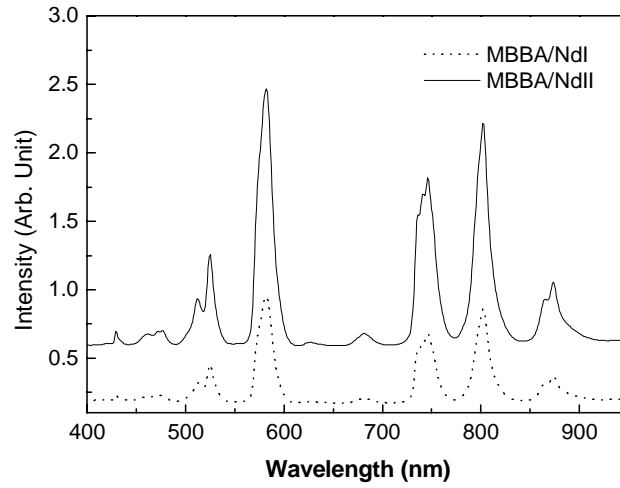


Fig. 1. Absorption spectra according to  $\text{Nd}^{3+}$  ion concentration

From the absorption spectra, absorption cross-section is calculated from Eq. (2)

$$\sigma_{abs} = \frac{2.303 \log \left( \frac{I_0}{I} \right)}{NL} \quad (2)$$

where  $N$  is  $\text{Nd}^{3+}$  ion concentration ( $\text{ion}/\text{cm}^3$ ),  $L$  is the thickness of the sample. The integrated absorption cross sections are calculated using the spectroscopic parameters from absorption spectra for the MBBA/NdI and the MBBA/NdII. The spectroscopic parameters in detail are presented in Table 1. The refractive index of the MBBA system increases when  $\text{Nd}^{3+}$  ion concentration increases. The increase of refractive index is mainly due to the dense packing of rare earth materials. The effects of rare earth dopant on optical properties are presented in previous works [5]. The absorption cross

section of the peak at the  ${}^4I_{9/2} \rightarrow {}^4F_{5/2}$  transition decreases with increasing  $\text{Nd}^{3+}$  ion concentration. The  ${}^4I_{9/2} \rightarrow {}^4F_{5/2}$  transition is particularly important because the transition has been used for laser diode pumping. The fluorescence lifetime also decrease from 168 $\mu\text{s}$  to 141 $\mu\text{s}$  when  $\text{Nd}^{3+}$  ion concentration increases. The decrease of fluorescence lifetime is mainly due to ion clustering.

Table 1. Spectroscopic parameters and absorption cross section for pump transition

Parameters	Unit	MBBA/NdI	MBBA/NdII
$\text{Nd}^{3+}$ dopant concentration ( $M$ )	$\times 10^{20} \text{ cm}^{-3}$	2.5	6.26
Refractive index ( $n_d$ )	-	1.5786	1.5847
Refractive index at transition wavelength: ${}^4I_{9/2} \rightarrow {}^4F_{5/2}$	-	1.5846	1.5891
Mean absorption wavelength ( $\lambda_p$ ) for the ${}^4I_{9/2} \rightarrow {}^4F_{5/2}$ transition	nm	802	802
Absorption cross section ( $\sigma_{abs}$ ) for pump ${}^4I_{9/2} \rightarrow {}^4F_{5/2}$	$\times 10^{20} \text{ cm}^2$	3.95	3.15
Integrated absorption cross section ( $\int \sigma_{abs}$ ) for pump ${}^4I_{9/2} \rightarrow {}^4F_{5/2}$	$\times 10^{31} \text{ pm}^3$	13.56	6.84
Fluorescence lifetime: measured ( $\tau$ )	$\mu\text{s}$	168	141

### 3.2 Emission properties

The radiative transition probabilities, are given in Eq. (3), were obtained with the line strength for the excited  ${}^4F_{3/2}$  to  ${}^4I_J$  manifold for  $\text{Nd}^{3+}$ .

$$A_{rad}[(S, L)J; (S', L')J'] = \frac{64\pi^4}{3h(2J+1)\lambda^3} \left[ \frac{n(n^2+2)^2}{9} \right] S_{ed} \quad (3)$$

where  $n(n^2+2)^2/9$  is the local field correction for  $\text{Nd}^{3+}$  in the initial  $J$  manifold.  $J'$  is the final manifold.  $n$  is the refractive index at the wavelength ( $\lambda$ ) of the transition determined by using Cauchy's equation,  $n(\lambda) = A + B/\lambda^2$ . The detail results on Judd-Ofelt parameters for  $\text{Nd}^{3+}$  ion in MBBA systems were referred to previous study [6]. The stimulated emission cross-section between  ${}^4I_J \rightarrow {}^4I_{J'}$  having measured lifetime ( $\tau_p$ ) is given by Fuchtbauer-Ladenburg method [7] as below

$$\sigma_{em} = \frac{\lambda_p^4}{8\pi c n (\lambda_p)^2 \Delta\lambda_{eff}} A \left[ ({}^4F_J); ({}^4F_{J'}) \right] \quad (4)$$

where  $\lambda_p$  is the wavelength of the peak emission,  $c$  is the speed of light in vacuums, and  $n(\lambda_p)$  is the refractive index at each emission peak wavelength.  $\Delta\lambda_{eff}$  is an effective linewidth. Since the emission band is asymmetry, it is used instead of the full width at half maximum linewidth. It is characterized in the name of an effective linewidth as below

$$\Delta \lambda_{eff} = \int \frac{I(\lambda)d\lambda}{I_{max}} \quad (5)$$

$I_{max}$  is the maximum intensity at fluorescence emission peaks. Fig.2 shows the emission spectra at around 1056nm and 1330nm emission peaks. The relative intensities are to a degree decreased with  $Nd^{3+}$  ion concentration. The spectra around 1330nm are shown in Fig 2 (b). The emission spectra were splitted to 1330nm and 1384nm more obviously. The splitting of emission spectra around 1350nm are not clearly lightened but the confidential interpretation on the splitting of emission spectra is that there exists a site competition among  $Nd^{3+}$  ions in an excited state [8].

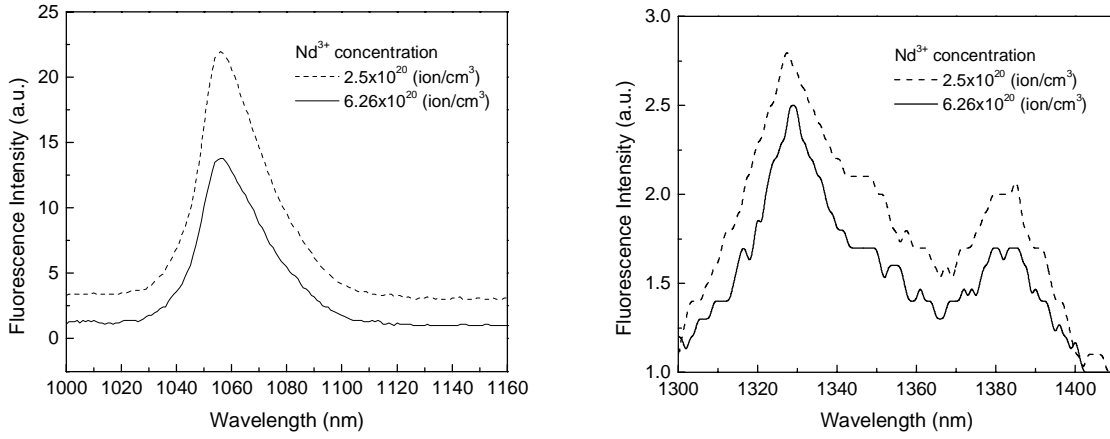


Fig. 2. Emission spectra of MBBA system according to  $Nd^{3+}$  ion concentration around (a) 1056nm (b) 1330nm

Various spectroscopic properties are listed in Table. 2 to evaluate emission properties. The emission peaks due to  ${}^4F_{3/2} \rightarrow {}^4I_{13/2}$  transition were shifted a little bit to longer wavelength with increase of  $Nd^{3+}$  ions. It indicates that host materials with excess  $Nd^{3+}$  doping affect the local field of  $Nd^{3+}$  ion. Generally the shift to longer wavelengths in glass is possibly related to the high refractive index and its relatively covalent bonding [5, 9].

The effective emission line width for the  ${}^4F_{3/2} \rightarrow {}^4I_{13/2}$  transition increased 36.1 to 32 for the MBBA/NdI and the MBBA/NdII, respectively. The emission cross section ( $\sigma_{em}$ ) for both  ${}^4F_{3/2} \rightarrow {}^4I_{13/2}$  and  ${}^4F_{3/2} \rightarrow {}^4I_{11/2}$  transition increased with  $Nd^{3+}$  ion concentration. The increase of the stimulated emission cross section is mainly due to the narrower effective linewidth for the MBBA/NdI and the MBBA/NdII. The laser performance is evaluated by considering stimulated emission cross-section ( $\sigma_{em}$ ) and the extraction efficiency ( $\tau * \sigma_{em}$ ). i.e. the figure of merit (FOM) for amplifier gain.

In this work, the extraction efficiency for  $Nd^{3+}$  ion in MBBA was recorded in the range of 1.91-2.31 for  ${}^4F_{3/2} \rightarrow {}^4I_{13/2}$  and of 6.18-9.41 for  ${}^4F_{3/2} \rightarrow {}^4I_{11/2}$  with  $Nd^{3+}$  ion concentration. Even the measured lifetimes ( $\tau$ ) decreased from 168 to 141 ( $\mu s$ ),

the figure of merit for amplifier gain was enhanced due to high integrated emission cross section and the narrowing of an effective linewidth.

Table 2. Spectroscopic properties on MBBA system doped with Nd<sup>3+</sup> ion

Glasses	Transition	Nd <sup>3+</sup> ion (x10 <sup>20</sup> , cm <sup>-3</sup> )	$\lambda_{em}$ (nm)	$A_{rad}$ (s <sup>-1</sup> )	$\Delta\lambda_{eff}$ (nm)	$\sigma_{em}$ (x10 <sup>4</sup> , pm <sup>2</sup> )	$\tau_r^* \sigma_{em}$ (s·pm <sup>2</sup> )
MBBA system	$^4F_{3/2} \rightarrow ^4I_{13/2}$	2.5	1328	247.16	36.1	1.14	1.91
		6.3	1330	246.04	25	1.64	2.31
	$^4F_{3/2} \rightarrow ^4I_{11/2}$	2.5	1056	1783.53	32	3.68	6.18
		6.3	1057	1778.53	17.7	6.68	9.41

#### 4. CONCLUSION

The stimulated emission cross section ( $\sigma_{em}$ ) and the extraction efficiency ( $\tau_r^* \sigma_{em}$ ) for Nd<sup>3+</sup> ion in MBBA system have been investigated. The stimulated emission cross section ( $\sigma_{em}$ ) for the  $^4F_{3/2} \rightarrow ^4I_{13/2}$  transition has been found to increase from 1.14 to 1.64 (x10<sup>4</sup> cm<sup>2</sup>) and for the  $^4F_{3/2} \rightarrow ^4I_{13/2}$  transition from 3.68 to 6.68 (x10<sup>4</sup> cm<sup>2</sup>) for MBBA/NdI (2.50x10<sup>+20</sup> cm<sup>-3</sup>) and MBBA/NdII (6.26x10<sup>+20</sup> cm<sup>-3</sup>), respectively. The increase of the stimulated emission cross section is mainly due to the narrower effective linewidth with Nd<sup>3+</sup> ion concentration. The extraction efficiency ( $\tau_r^* \sigma_{em}$ ) for Nd<sup>3+</sup> ion in MBBA is found to be in the range of 1.91-2.31 for  $^4F_{3/2} \rightarrow ^4I_{13/2}$  and of 6.18-9.41 for  $^4F_{3/2} \rightarrow ^4I_{11/2}$  with Nd<sup>3+</sup> ion concentration, respectively. The enhancement of spectroscopic properties with Nd<sup>3+</sup> ion concentration suggests some potential for laser applications using two characteristic emissions.

#### REFERENCES

1. C. Brecher, L.A. Riseberg, *Phys. Rev. B18*, pp.5799, 1978
2. S. V. J. Lkshmn, Y.C. Ratnkaran, *Phys. Chem. Glasses* 29, pp.26, 1988
3. B. Viana, M. Palazzi, O. LeFol, *J. Non-Cryst. Solids* 215, pp.96, 1997
4. S. Jiang, T. Luo, B. C. Hwang, F. Smekatala, K. Seneschal, J. Lucas, N. Peyghambarian, *J. Non-Cryst. Solid*, 263-264, pp.364-368, 2000
5. Ju H. Choi, F. G. Shi, A. Margaryan, A. Margaryan, (4970-11, *Photonic west, Jan. 2003 San Jose*)
6. Ju H. Choi, F. G. Shi, A. Margaryan, A. Margaryan, (4974-20, *Photonic west, Jan. 2003 San Jose*)
7. S.A. Payne, L.L. Chase, L.K. Smith, W.L. Kway, W.F. Kruke, *IEEE J. Quantum Electron.* 28, pp.2619, 1992
8. F. Gan, *SPIE Vol. 3416*, pp.134-143, 1998
9. D.K. Sardar, F. Castano, J. French, J.B. Gruber, T. A. Reynolds, T. Alekel, D. A. Keszler, B.L. Clark, *J. Appl. Phys.*, Vol. 90, No 10, pp.4997-5001, 2001